Supporting Information

Effect of Single-Site Charge-Reversal Mutations on the Catalytic Properties of Yeast Cytochrome *c* Peroxidase: Mutations Near the High-Affinity Cytochrome *c* Binding Site

Naw May Pearl, Timothy Jacobson, Moraa Arisa, Lidia B. Vitello, and James E. Erman

Department of Chemistry and Biochemistry, Northern Illinois University, DeKalb, IL 60115

Tables and figures in the Supporting Information will be designated S1, S2, S3, etc. References to tables and figures without the S prefix refer to tables and figures in the published article.

Locations of the Charge-Reversal Mutations. Figures S1, S2, and S3 show the locations of the 15 mutation sites used in this study to investigate the effect of charge-reversal mutations on the catalytic properties of CcP. The 15 mutation sites are on the front-face of CcP, the face defined by the high-affinity cytochrome *c* binding site identified in the crystallographic structure of the yeast iso-1cytochrome *c*/CcP complex (1).

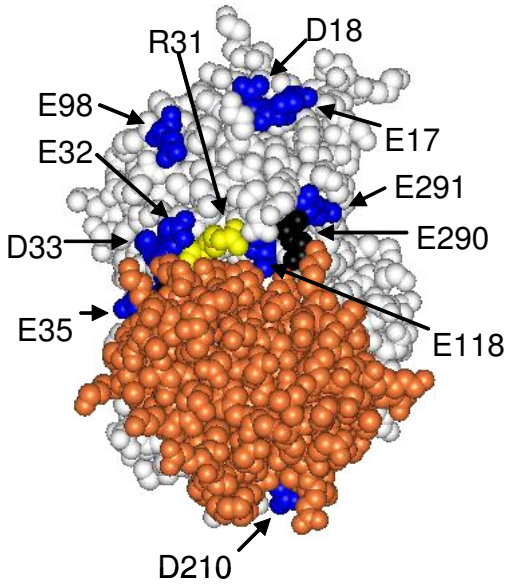

Figure S1. Space-filling model of the yeast cytochrome *c*/CcP complex (1). Yeast cytochrome *c* (red) is shown in front of the CcP molecule. CcP is shown in white with the locations of the aspartate and glutamate residues to be converted to lysines shown in blue. The Arg-31 site is shown in yellow. Glu-290 is one of the residues that define the cytochrome *c* binding site and is shown in black. Only those mutation sites visible in this view are labeled. The orientation of the CcP molecule is the same as that shown in Figure 1 of the published article.

Figure S1 shows the yeast iso-1 cytochrome *c*/CcP complex in the same orientation as the CcP molecule shown in Figure 1 of the published article, except that the cytochrome *c* molecule is shown in place. In this view only eleven of the mutation sites are visible. Asp-34, Glu-201, and Glu-209 are obscured by cytochrome *c* and Asp-37 is located behind the visible surface on the left-hand side of CcP.

Figure S2 shows the cytochrome *c*/CcP complex in the same orientation as in Figure S1 except that the complex is rotated 90º in a counter-clockwise direction about a vertical axis. The view in Figure S2 shows the left-hand face of CcP. The color labeling is the same as in Figure S1. Two residues not visible in Figure S1 are seen in this view, Asp-37 and Ala-193. Ala-193 is one of the residues that define the cytochrome *c* binding site and is shown in black. Ala-193 is

located toward the lower edge of the cytochrome *c* binding site. The lower front-face of the CcP molecule and the lower portion of the bound cytochrome *c* molecule diverge from one another below Ala-193. In this view, it is apparent that Glu-17, Asp-18, Asp-37, and Asp-210 are somewhat distant from the bound cytochrome *c* molecule.

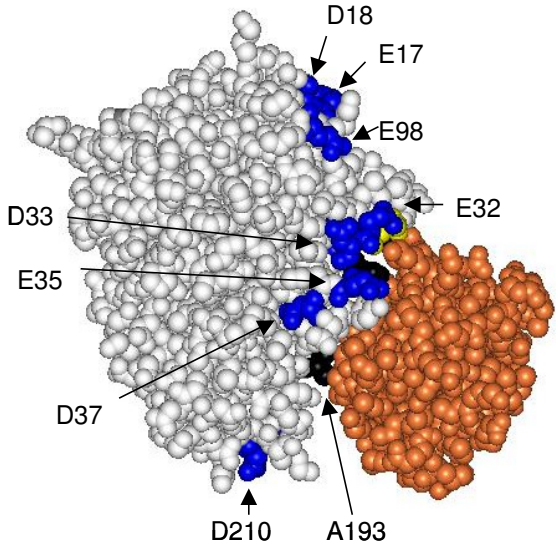

Figure S2. Space-filling model of the yeast cytochrome *c*/CcP complex (S1). The orientation of the complex is the same as in Figure S1 except that it is rotated 90º counter clockwise about a vertical axis, showing the left-hand face of CcP and the bound cytochrome *c*. The color scheme is the same as in Figure S1. Asp-37 and Ala-193 are observed in this view while they were not visible in Figure S1. Ala-193 is one of the three residues used to define the cytochrome *c* binding site and is shown in black.

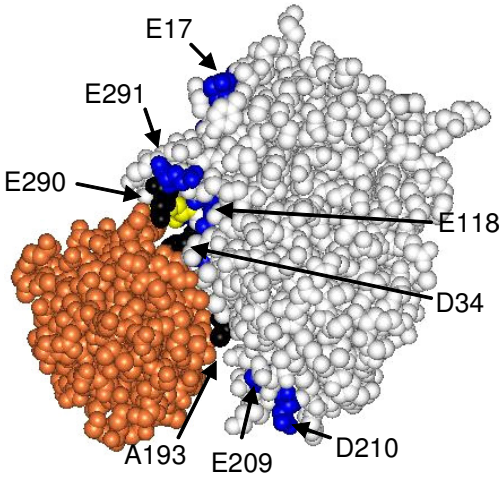

Figure S3. Space-filling model of the yeast cytochrome *c*/CcP complex (S1). The orientation of the complex is the same as in Figure S1 except that it is rotated 90º clockwise about a vertical axis, showing the right-hand-face of CcP and the bound cytochrome *c*. The color scheme is the same as in Figure S1. Glu-209 is observed in this view.

Figure S3 shows the cytochrome *c*/CcP complex in the same orientation as in Figure S1 except that the complex is rotated 90º in a clockwise direction about a vertical axis showing the right-hand face of the CcP molecule. Glu-209 is visible in this view but not in Figures S1 and S2. The three residues that define the cytochrome *c* binding site, Asp-34, Ala-193, and Glu-290 are visible in Figure S3. Asp-34 is in the background of crevice occurring between CcP and cytochrome *c* in the upper portion of the interface between the two proteins.

Spectra of the Charge-Reversal Mutations at pH 6.0 and 7.5. The spectra of all charge reversal mutations were determined at pH 6.0 and 7.5 in 0.100 M ionic strength, potassium phosphate buffers. The spectra provide the first characterization of the mutants including a measure of the purity index as well as giving an indication of the presence or absence of six-coordinate heme forms in the samples at both pH 6.0 and 7.5. The spectra of rCcP and all 15 mutants are shown in Figures S4 through S19.

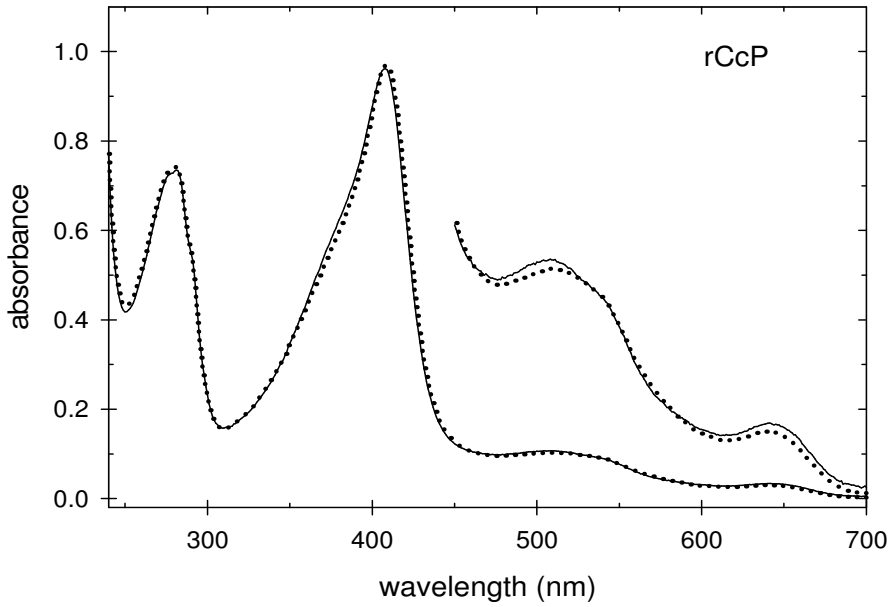

Figure S4. Spectrum of rCcP at pH 6.0 (solid line) and pH 7.5 (dotted line). The visible region of the spectrum is expanded by a factor of 5.

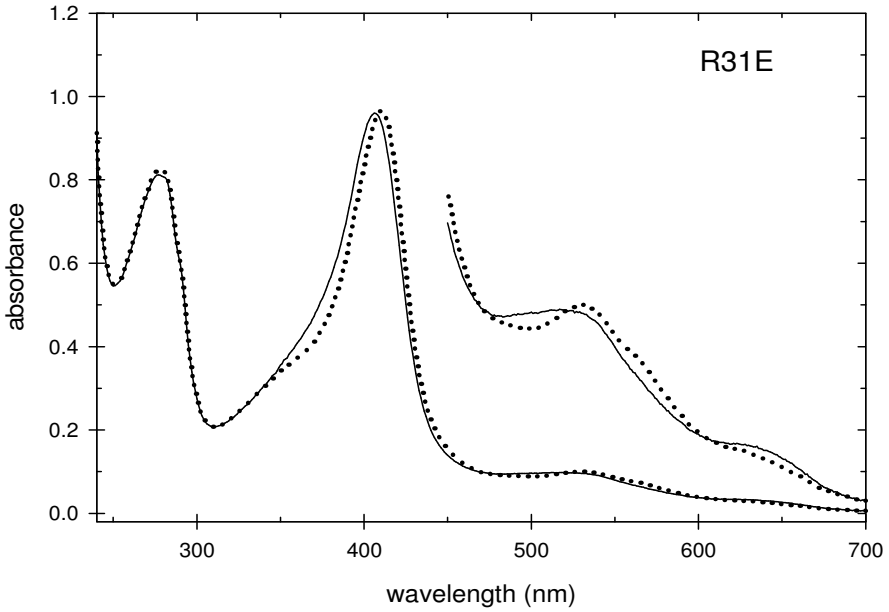

Figure S5. Spectrum of R31E at pH 6.0 (solid line) and pH 7.5 (dotted line). The visible region of the spectrum is expanded by a factor of 5.

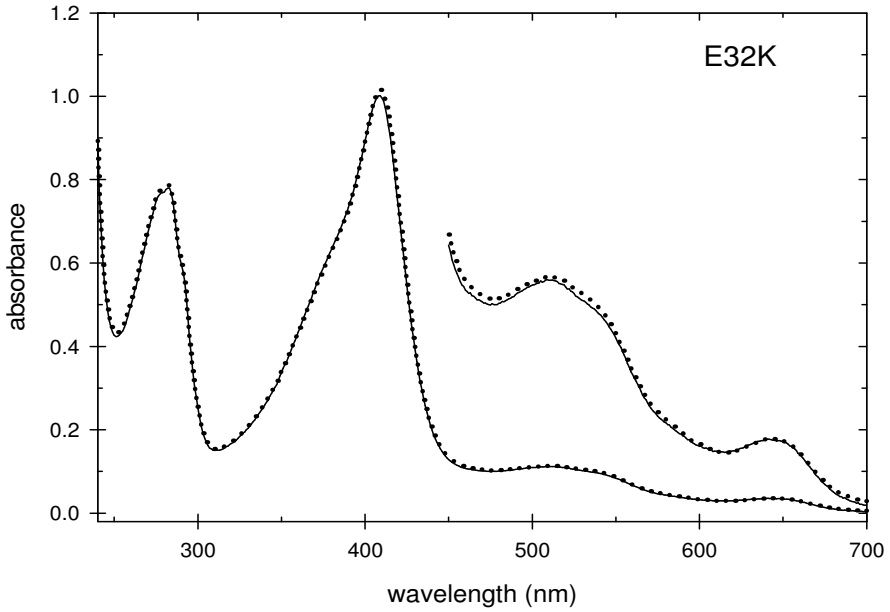

Figure S6. Spectrum of E32K at pH 6.0 (solid line) and pH 7.5 (dotted line). The visible region of the spectrum is expanded by a factor of 5.

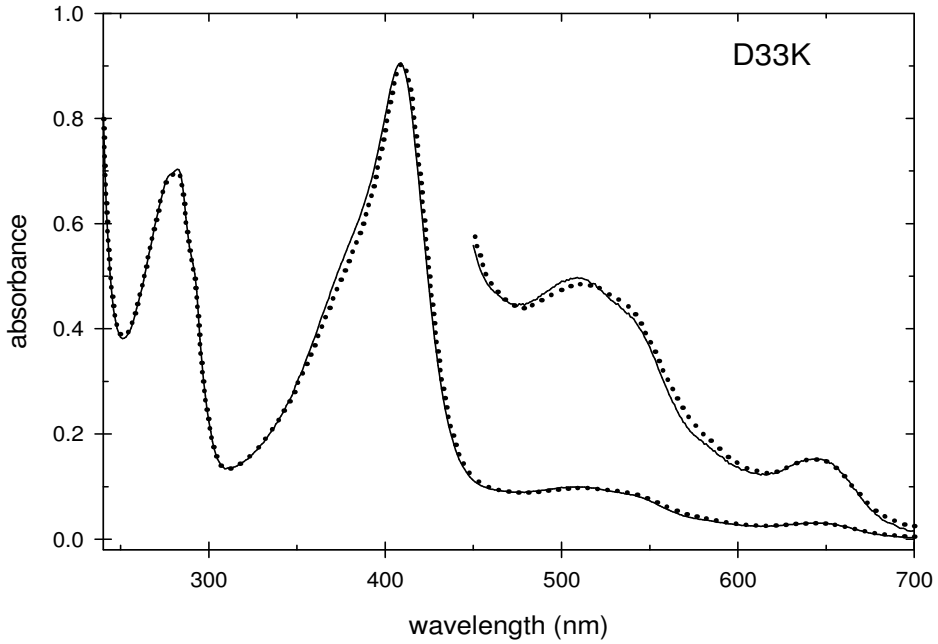

Figure S7. Spectrum of D33K at pH 6.0 (solid line) and pH 7.5 (dotted line). The visible region of the spectrum is expanded by a factor of 5.

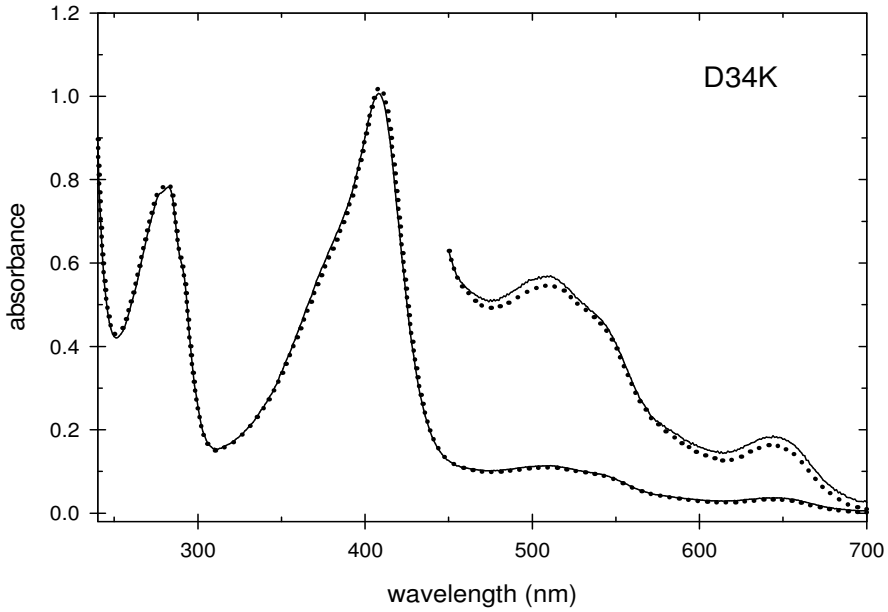

Figure S8. Spectrum of D34K at pH 6.0 (solid line) and pH 7.5 (dotted line). The visible region of the spectrum is expanded by a factor of 5.

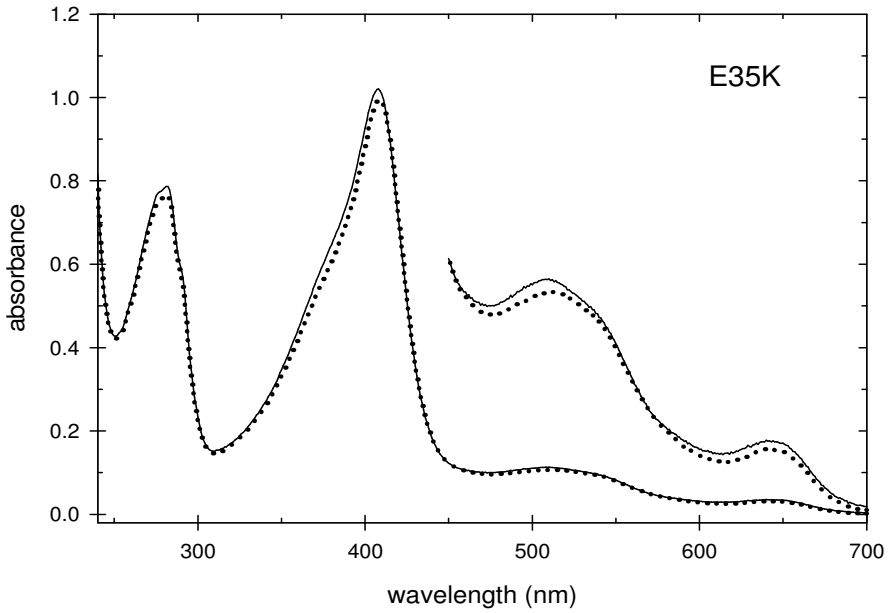

Figure S9. Spectrum of E35K at pH 6.0 (solid line) and pH 7.5 (dotted line). The visible region of the spectrum is expanded by a factor of 5.

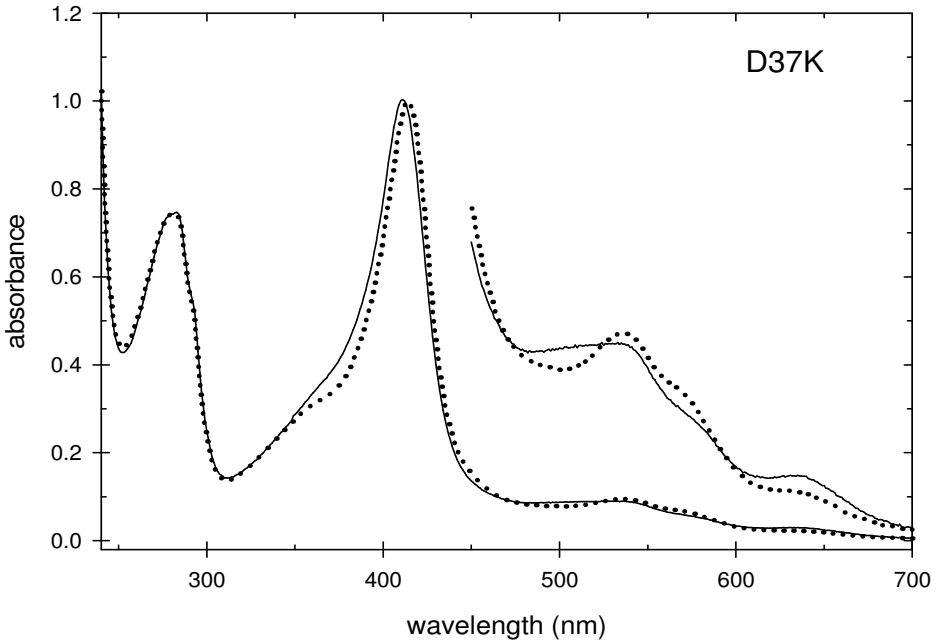

Figure S10. Spectrum of D37K at pH 6.0 (solid line) and pH 7.5 (dotted line). The visible region of the spectrum is expanded by a factor of 5.

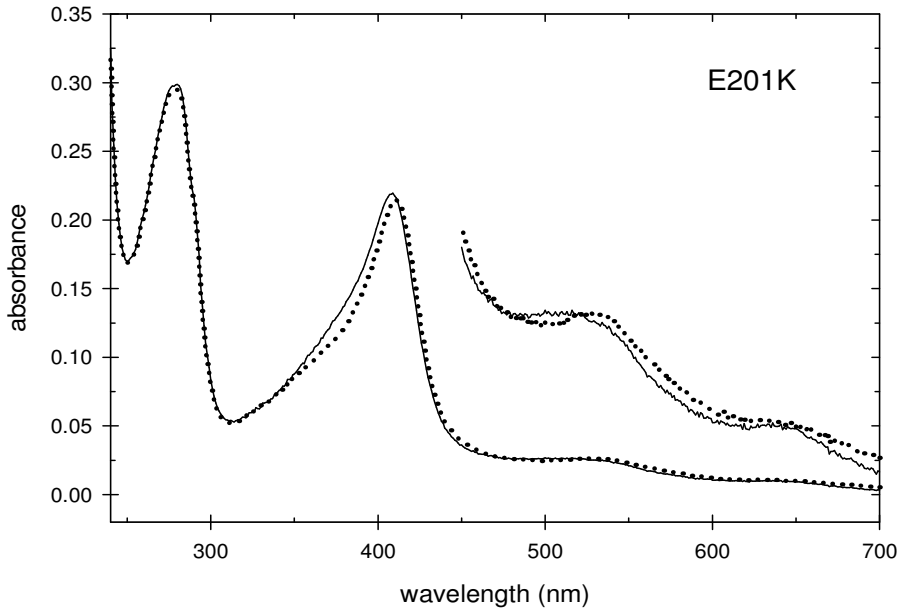

Figure S11. Spectrum of E201 at pH 6.0 (solid line) and pH 7.5 (dotted line). The visible region of the spectrum is expanded by a factor of 5.

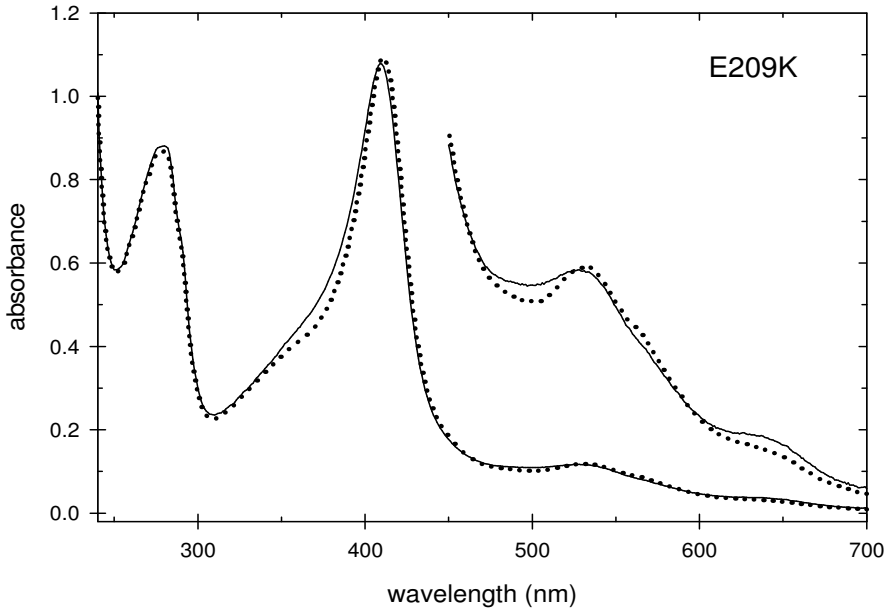

Figure S12. Spectrum of E209 at pH 6.0 (solid line) and pH 7.5 (dotted line). The visible region of the spectrum is expanded by a factor of 5.

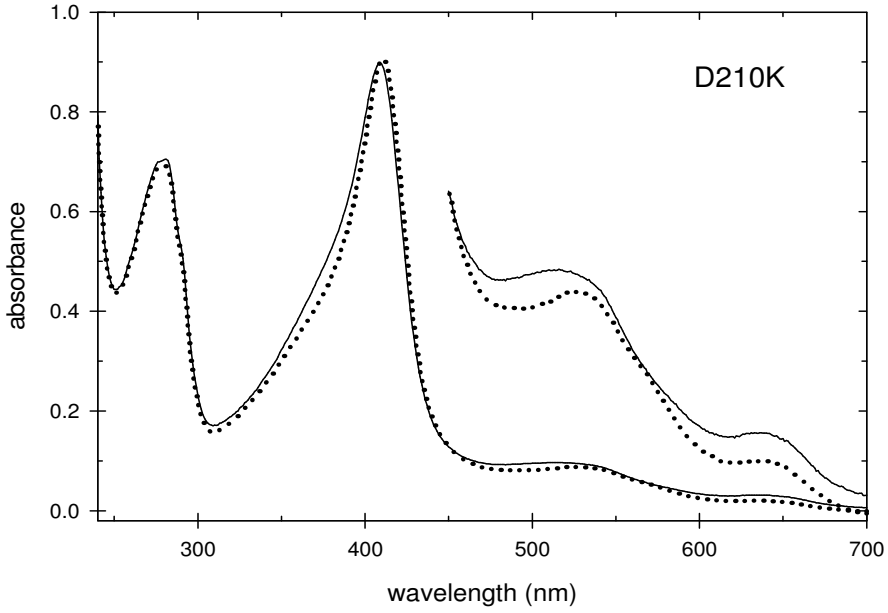

Figure S13. Spectrum of D210K at pH 6.0 (solid line) and pH 7.5 (dotted line). The visible region of the spectrum is expanded by a factor of 5.

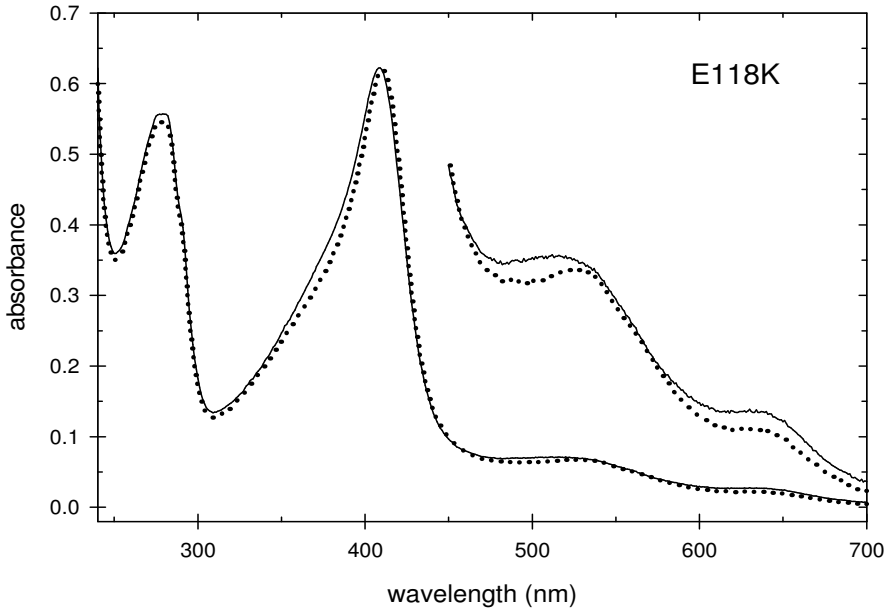

Figure S14. Spectrum of E118K at pH 6.0 (solid line) and pH 7.5 (dotted line). The visible region of the spectrum is expanded by a factor of 5.

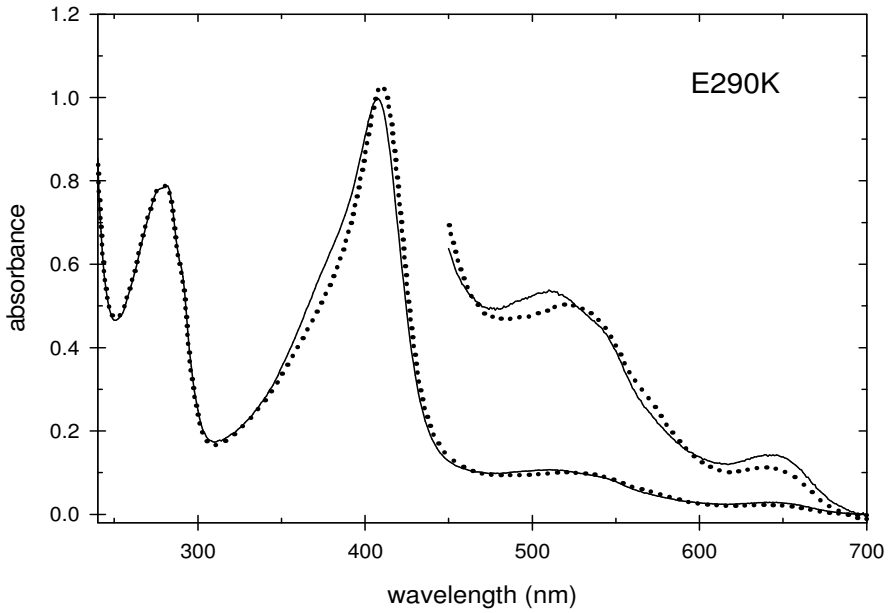

Figure S15. Spectrum of E290K at pH 6.0 (solid line) and pH 7.5 (dotted line). The visible region of the spectrum is expanded by a factor of 5.

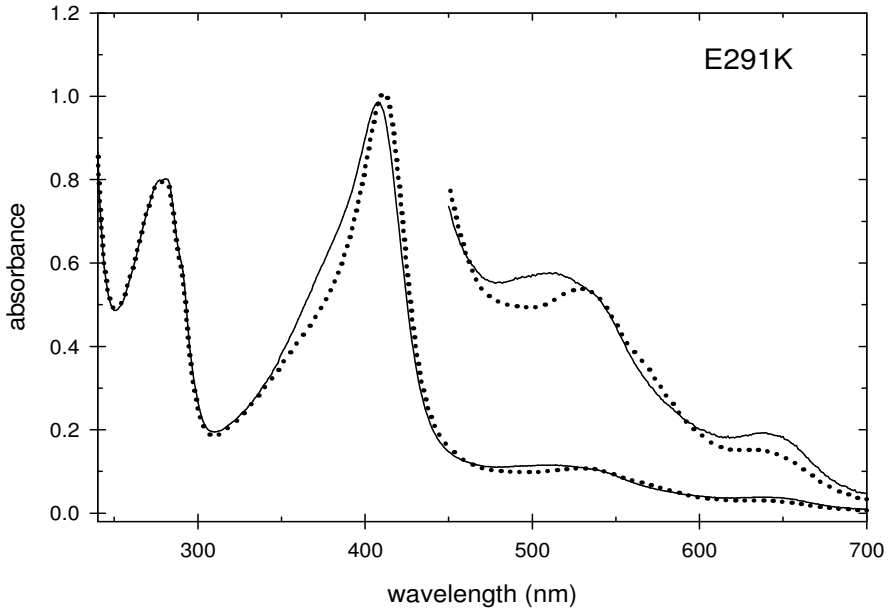

Figure S16. Spectrum of E291K at pH 6.0 (solid line) and pH 7.5 (dotted line). The visible region of the spectrum is expanded by a factor of 5.

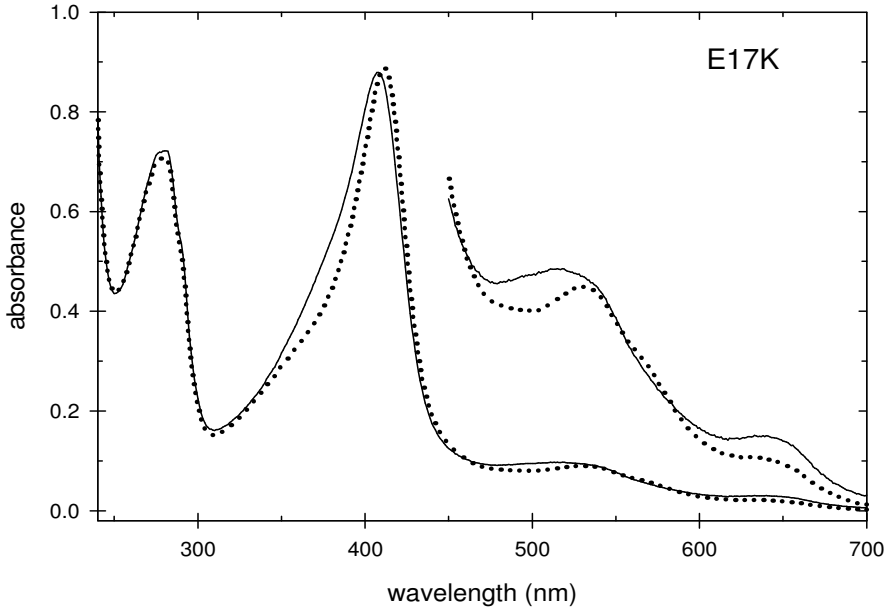

Figure S17. Spectrum of E17K at pH 6.0 (solid line) and pH 7.5 (dotted line). The visible region of the spectrum is expanded by a factor of 5.

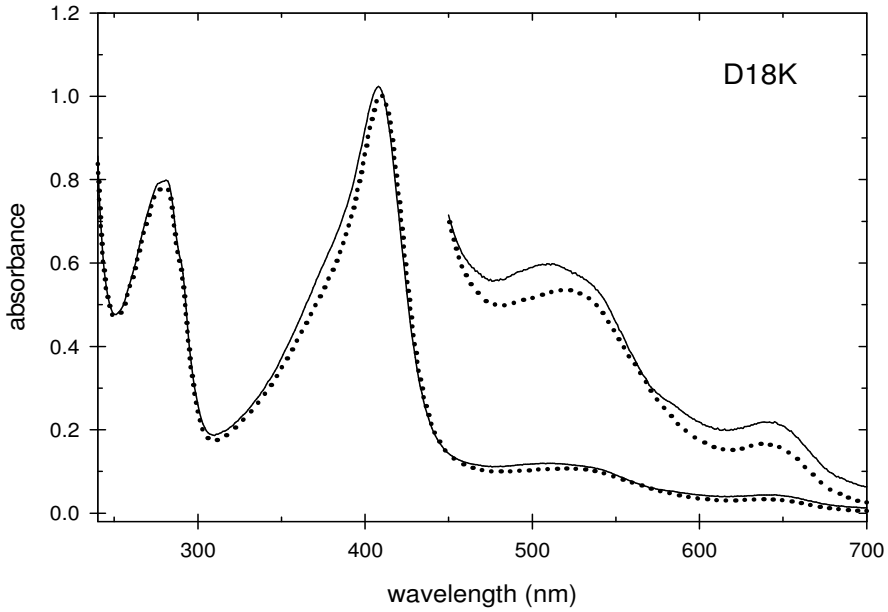

Figure S18. Spectrum of D18K at pH 6.0 (solid line) and pH 7.5 (dotted line). The visible region of the spectrum is expanded by a factor of 5.

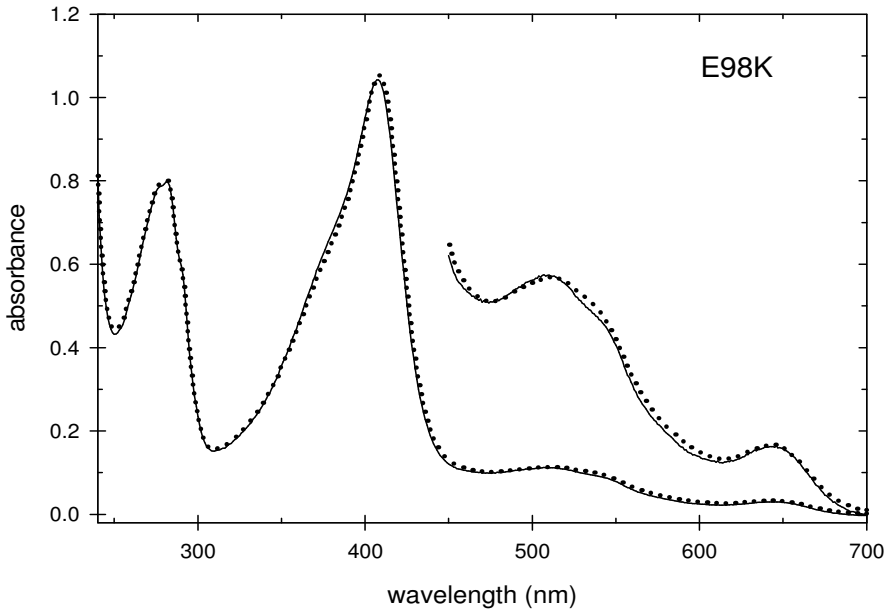

Figure S19. Spectrum of E98K at pH 6.0 (solid line) and pH 7.5 (dotted line). The visible region of the spectrum is expanded by a factor of 5.

Effect of Charge-Reversal Mutations on the Spectrum of CcP. The spectra of yCcP, CcP(MI), and rCcP are essentially independent of pH between pH 4 and 7 in the absence of buffer components that bind in the heme pocket such as high concentrations of acetate and nitrate (2-4). In this pH region, the heme group of CcP is predominantly five-coordinate and high-spin. Changes in the absorption spectrum are detectable above pH 7.0 (3, 4) as CcP begins to undergo a complex series of transformations at alkaline pH leading to formation of two distinct low-spin forms of CcP, followed by complete denaturation of the enzyme at pH 12 (5, 6). The absorption spectra of the two low-spin forms of CcP observed at alkaline pH are consistent with a hydroxy-ligated heme and a form in which His-52 is coordinated to the heme iron (6). The five- and six-coordinate species exist in a pH-dependent equilibrium with an apparent pK_A of 9.7 with the five-coordinate form predominating at low pH and the six-coordinate forms predominating at high pH (5). Hexa-coordinate heme is seen at lower pH values in some of the charge-reversal mutants than in wild-type CcP. Potential heme ligands include water, the hydroxide ion, and the imidazole group of the distal histidine, His-52.

The changes in the spectral properties of the charge-reversal mutants documented in Table 1 are associated with the pH-dependent change in heme ligation and spin-state. The changes in the absorption spectrum at pH 7.5 relative to those at pH 6.0 include a red-shift in the position of the Soret band and a decrease in the absorbance at the δ band position near 380 nm relative to that at the Soret maximum, Table 1. The average red-shift in the Soret maximum for the eighteen entries in Table 1 is about 2 nm, ~408 to ~410 nm, between pH 6 and 7.5. The ratio of the Soret absorbance to the absorbance at 380 nm can be used as an indicator of five- and six-coordination. The heme group in yCcP at pH 6 is essentially 100% five-coordinate, high-spin and the A_{Soret}/A_{380} ratio is 1.52 ± 0.04 for a large number of isolates (2). The A_{Soret}/A_{380} ratio varies between 2.4 and 3.7 for authentic six-coordinate, low-spin CcP species including the CcP/cyanide complex (7), the two alkaline CcP low-spin species (5), and two low-spin species observed in the CcP(D235N) mutant (6). For the charge-reversal mutations, the A_{Soret}/A_{380} ratio varies between 1.53 and 2.23 at pH 6.0, and between 1.62 and 2.59 at pH 7.5, Table 1.

It is interesting to observe that a surface mutation, such as the D37K mutation, can affect coordination of the buried heme group. Spectra of the D34K and D37K mutants are shown in Figure 2 to demonstrate the variation in spectral parameters observed at pH 6.0. The D34K mutant has a spectrum very similar to that of yCcP and rCcP while that of the D37K mutant is influenced by significant amounts of hexa-coordinate heme.

At pH 7.5, the A_{Soret}/A_{380} ratio is larger than the ratio at pH 6.0 for all the proteins included in Table 1 indicating a higher concentration of six-coordinate forms at the higher pH. The increase in hexa-coordinate forms at pH 7.5 compared to pH 6.0 is most likely due to the perturbation of the apparent pK_A for the five- to six-coordinate transition in the charge-reversal mutants compared to that in yCcP. Electrostatic considerations can be used to explain these results. The initial hexa-coordinate CcP species formed during the alkaline transition is thought to involve binding of a hydroxide ion to the heme in CcP (5, 6). Binding of hydroxide would change the net charge at the heme center from +1 in the five-coordinate, high-spin form to zero in the hydroxy-ligated species. Increasing the net charge on CcP by +2 through mutation of an aspartate or glutamate residue to a lysine residue would tend to destabilize the five-coordinate species, shifting the penta- to hexa-coordinate transition to lower pH.

***Steady-State Velocity Plots*.** Representative steady-state velocity plots for those mutants with significantly different catalytic parameters than rCcP are shown below. Figure S20 shows the data for mutants R31E and D34K, Figure S21 shows the data for D37K and E201K, while Figure S22 shows the data for E118K and E290K.

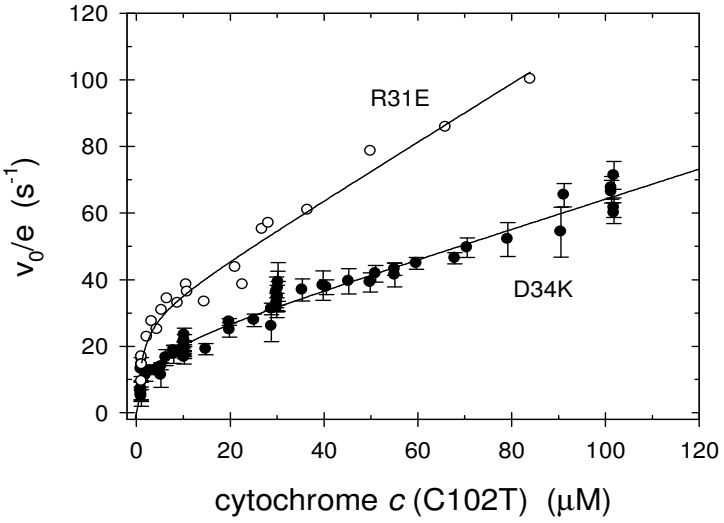

Figure S20. Steady-state velocities, v_0, as a function of the yeast iso-1 ferrocytochrome *c*(C102T) concentration for two rCcP mutants, R31E and D34K. Experimental conditions: 0.100 M ionic strength potassium phosphate buffer, pH 7.5, 25°C, [H_2O_2] = 200 μM.

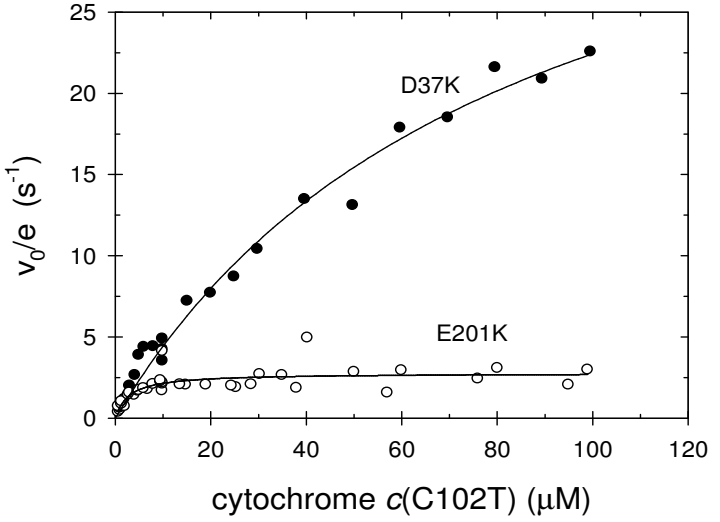

Figure S21. Steady-state velocities, v_0, as a function of the yeast iso-1 ferrocytochrome *c*(C102T) concentration for two rCcP mutants, D37K and E201K. Experimental conditions: 0.100 M ionic strength potassium phosphate buffer, pH 7.5, 25°C, [H_2O_2] = 200 μM.

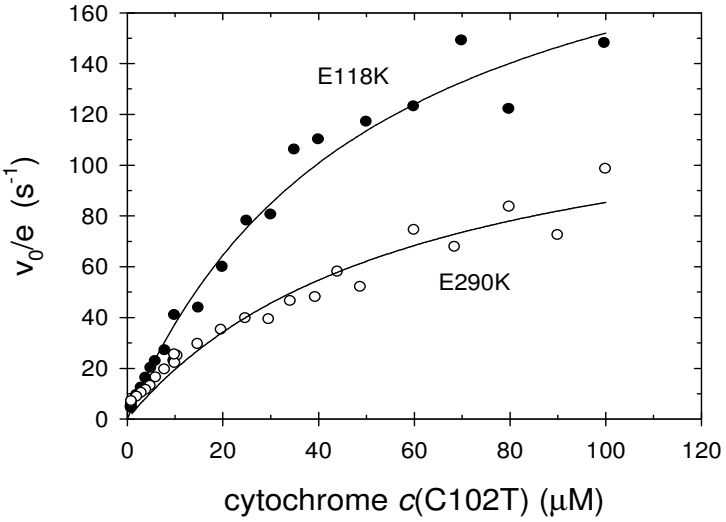

Figure S22. Steady-state velocities, v_0, as a function of the yeast iso-1 ferrocytochrome *c*(C102T) concentration for two rCcP mutants, E118K and E290K. Experimental conditions: 0.100 M ionic strength potassium phosphate buffer, pH 7.5, 25°C, [H_2O_2] = 200 μM.

Reaction with Hydrogen Peroxide at pH 6.0. The hydrogen peroxide stoichiometry and rates of the reaction, including rates for both the fast and slow phases where appropriate are tabulated in Table S1 for data collected at pH 6.0.

Slow Kinetic Phase of the Reaction between H_2O_2 and the Charge-Reversal Mutants. We have previously reported that some, but not all, preparations of yCcP show biphasic kinetics (2, 8). We only observe the slow phase of the reaction at pH 6 or below and the amplitude of the reaction is generally less than 2% of the total absorbance change for the hydrogen peroxide reaction at 424 nm. The rate of the slow phase is ~2 s^{-1} at 25 ºC, independent of the hydrogen peroxide concentration. Balny *et al.* (9) have studied the temperature dependence of the hydrogen peroxide/yCcP reaction and also observe biphasic kinetics under all experimental conditions. Balny *et al.* report that the rate for the slow phase of the reaction is independent of hydrogen peroxide concentration, that the rate increases with increasing pH, and the amplitude varies from about 20% of the total absorbance change at low pH to less than 2% at pH 8. Balny *et al.* report a rate of 0.14 s^{-1} at pH 6.1, 2ºC with an activation energy of 20.5 ± 0.2 kcal/mol (9).

We have observed the slow phase of the H_2O_2 reaction for fourteen of the fifteen mutants at pH 6.0, Table S1, and for eight of the mutants at pH 7.5, Table 3 (published paper). The slow phase of the reaction has a larger amplitude at pH 6.0 than at pH 7.5, consistent with our observations for wild-type CcP and with the data of Balny *et al*. (9). The amplitude of the slow phase ranges from 0 to 35% of the reaction amplitude at pH 6.0, averaging 15 ± 11% for the fifteen mutants. The average amplitude of the slow phase is 6 ± 3% for the eight mutants having

Table S1. Kinetic Parameters for Reaction of rCcP and Its Charge-Reversal Mutants with H_2O_2, pH 6.

	Fast Phase		Slow Phase			Inactive
Mutant	% Enzyme	k_1 ($\mu M^{-1}s^{-1}$)	% Enzyme	k_2 ($\mu M^{-1}s^{-1}$)	k_3 (s^{-1})	% Enzyme
yCcP	98	45 ± 3	2	-	~2	0
CcP(MI)	82	47 ± 4	15	-	8 ± 2	3
rCcP	81	47 ± 1	8	2.2 ± 0.1		11
Negative Cluster Mutants						
R31E	50	51 ± 3	28	2.5 ± 0.6	-	22
E32K	94	39 ± 7	6	1.5 ± 0.6	-	0
D33K	92	41 ± 4	8	-	34 ± 8	0
D34K	85	51 ± 12	12	-	27 ± 16	3
E35K	92	41 ± 9	8	2.0 ± 0.4	-	0
D37K	46	34 ± 5	9	-	14 ± 6	45
Mutants Near Ala-193						
E201K	61	36 ± 5	7	1.6 ± 0.2	-	32
E209K	38	29 ± 7	0	-	-	62
D210K	63	36 ± 7	8	-	23 ± 2	29
Mutants Near Glu-290						
E118K	54	25 ± 6	20	-	25 ± 11	26
E290K	56	38 ± 5	28	1.7 ± 0.2	-	16
E291K	40	30 ± 7	35	1.9 ± 0.1	-	25
Top Front-Face Mutants						
E17K	35	41 ± 7	37	2.0 ± 0.1	-	28
D18K	76	48 ± 1	13	2.5 ± 0.4	-	11
E98K	91	46 ± 7	9	-	35 ± 7	0

the slow phase of the reaction at pH 7.5, ranging from 2 to 10%. At pH 6.0, where fourteen of the fifteen mutants have a slow phase of the H_2O_2 reaction, the slow phase is independent of the hydrogen peroxide concentration for six of the mutants and dependent upon the H_2O_2 concentration for eight of the mutants, Table S1.

The rate constant for the hydrogen peroxide independent process, which we define as k_3, varies between ~2 s^{-1} for yCcP to 35 ± 7 s^{-1} for E98K, both at pH 6.0, Table S1. For the mutants that have a slow phase that is linearly dependent upon the hydrogen peroxide concentration, the bimolecular rate constant, defined as k_2, appears to be independent of pH and has an average value of 2.0 ± 0.4 μM^{-1} s^{-1}, over 20 times smaller than k_1.

Estimation of the Fraction of H_2O_2-Reactive Enzyme. During the study of the reaction between the charge-reversal mutants and H_2O_2, it became apparent that the absorbance changes upon reaction with H_2O_2 for some of the mutants were significantly smaller than for wild-type CcP. We attributed this to unreactive forms of the mutant enzymes.

We used the spectrum of the mutant enzyme in the presence of a slight excess of H_2O_2 (~20% stoichiometric excess) to estimate the fraction of H_2O_2-reactive enzyme. The estimate is based upon the assumption that the spectrum of Compound I in the mutant enzyme is identical to the spectrum of Compound I for yCcP. This should be a reasonable assumption since the heme ligation for the mutant enzyme Compound I should be the same as it is in yCcP Compound I, with His-175 coordinated to the fifth coordination site and the oxyferryl oxygen atom covalently bound to the sixth coordination site. However, the heme environment of the mutants may be somewhat different than that of yCcP and cause some perturbation of the Compound I spectrum. Evidence for perturbation of the Compound I spectrum comes from the observation that we obtain slightly different estimates of the fraction of active enzyme depending upon the wavelength chosen to do the calculation. We have systematically used the absorbance changes at 424 nm to estimate the active enzyme since the absorbance changes are ~10 times larger than those in the visible region and should be more reproducible.

Another caveat in using this method to estimate the amount of Compound I is that the Trp-191 cation radical may not be as stable in the charge-reversal mutants as it is in yCcP Compound I. There is the possibility of producing a classical peroxidase Compound I with a porphyrin cation radical rather than the Trp-191 radical such as we observed in the CcP(W191F) mutant (10). Additionally, the Trp-191 radical could decay rapidly leaving Compound II rather than Compound I, or both Compounds I and II could decay rapidly such that the amount of H_2O_2-reactive enzyme is underestimated. The data suggest that none of these possibilities occur. First, there is no evidence of a classical peroxidase Compound I with a radical on the heme ring and low Soret absorbance since even D37K, the mutant that gives the smallest amount of Compound I, shows a red-shift in the Soret band with an increase in absorbance at 424 nm and the formation of α and β bands at 560 and 530 nm, respectively, Figure 5, all characteristic of the Fe(IV) heme group and not the porphyrin radical. Second, we have measured formation of the mutant Compound I using stopped-flow techniques and these show an exponential rise to the final absorbance position at 424 nm that is observed in the manual-mixing experiments. It should be noted that the rapid formation of Compound I in the mutants occurs at the same rate as yCcP Compound I, Table 3 and Table S1. There is no indication of a rapid decay of Compound I in the stopped-flow experiments such that the manual mixing experiments, Figures 4 and 5, would underestimate the amount of Compound I.

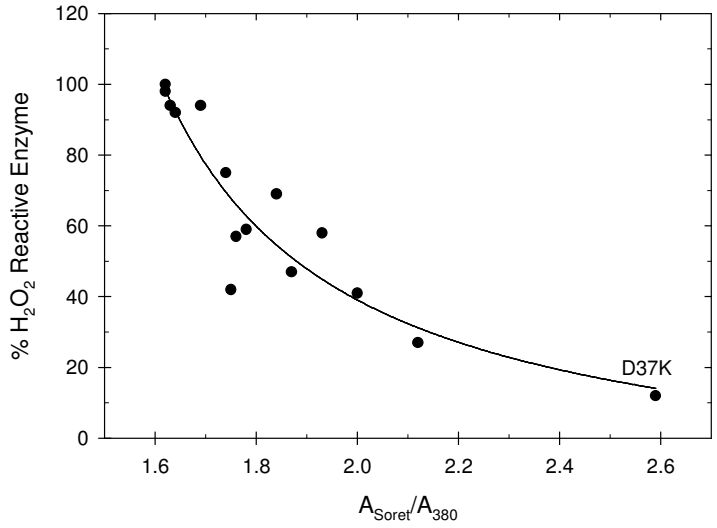

Figure S23. Correlation between the percentage of hydrogen peroxide-reactive enzyme for rCcP and the fifteen mutants used in this study as a function of the ratio of absorbance at the Soret maximum to that at 380 nm. The A_{Soret}/A_{380} ratio is an indirect measure of the amount of hexa-coordinate heme forms present in the rCcP and its mutants. The D37K mutant has the largest A_{Soret}/A_{380} ratio and only its position is labeled. All data collected at pH 7.5

Irrespective of the potential errors in estimating the fraction of active enzyme for the charge-reversal mutants, it is clear from the spectroscopic changes that some of the mutant enzymes have substantially altered reactivity toward hydrogen peroxide. This altered reactivity generally correlates with the amount of hexa-coordinate heme present in the mutants as monitored by the A_{Soret}/A_{380} ratio, Figure S23.

We have suggested above, that the predominant hexa-coordinate form of CcP has a hydroxide ion coordinated to the sixth coordination site of the heme iron and that the distribution of charges on the surface of CcP can change the relatively stabilities of the penta- and hexa-coordinate forms of the heme, shifting the apparent pK_A for the alkaline transition in CcP. The observation that the hexa-coordinate forms of CcP and CcP mutants do not react with H_2O_2 requires that the equilibration rate between the penta- and hexa-coordinate forms of the heme to be very slow compared to the rate of reaction between H_2O_2 and the penta-coordinate heme, otherwise, as the penta-coordinate form is depleted during conversion to Compound I, the hexa-coordinate form would equilibrate to replenish the penta-coordinate form and eventually all of the enzyme would be converted to Compound I. This does not happen during the time frame of the experiments described here. The non-reactivity of the hexa-coordinate, alkaline forms of both yCcP and CcP(MI) has been reported previously (4). Wild-type yCcP reacts stoichiometrically with H_2O_2 between pH 4 and 7 to form Compound I but at pH 7.5 and above the fraction of yCcP that reacts with H_2O_2 decreases as the native penta-coordinate form is converted to unreactive hexa-coordinate forms at alkaline pH. The H_2O_2 titer for yCcP decreases from 1.01 ± 0.05 between pH 4 and 7 to 0.96 ± 0.05 at pH 7.5 and 0.78 ± 0.07 at pH 8.0 (4).

Correlation of the Fraction of H_2O_2-Reactive Enzyme and V_{max}/e_0. As mentioned in the paper, the large variation in the maximum turnover rates of the charge-reversal mutations was

unexpected. The observation that the charge-reversal mutations can affect heme ligation in the mutants and that the hexa-coordinate heme forms do not react with H_2O_2, Figure S23, provide a rationale for most of the variation in V_{max}/e_0 observed in the mutants. Figure S24 shows a plot of the maximum turnover number of the charge-reversal mutants as a function of the estimated fraction of inactive enzyme within each mutant. In general, as the percentage of H_2O_2- inactive enzyme increases, the maximum turnover number decreases.

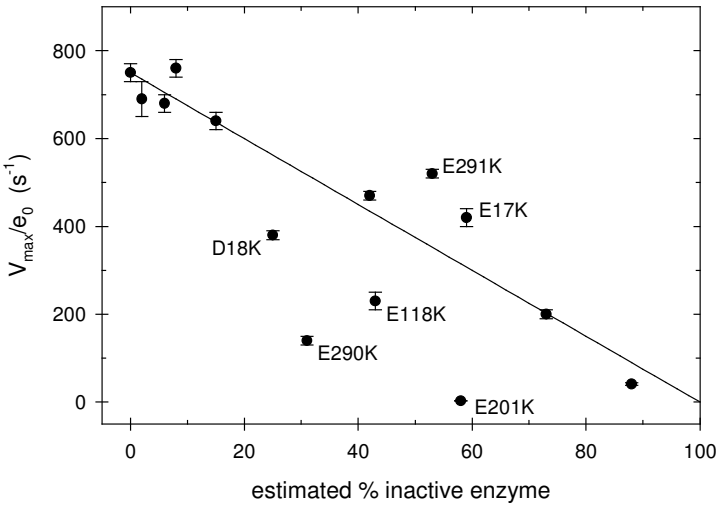

Figure S24. Plot of the maximum turnover rate of the charge-reversal mutants as a function of the estimated percentage of H_2O_2-reactive enzyme. The solid line is calculated based on a V_0/e_0 value of 750 s^{-1} for fully active enzyme. Mutants with significant deviation from the correlation line are identified in the figure.

The calculated line in Figure S24 is for the condition that the maximum turnover rate is directly proportional to the percentage of enzyme that reacts with hydrogen peroxide. This correlation also requires that Compound I formed by the mutants is fully active in oxidizing the substrate, ferrocytochrome *c*. As can be seen in Figure S24, the correlation is not perfect. One reason could be due to errors in estimating the fraction of inactive enzyme discussed above but it is also possible that some of the mutants do not oxidize ferrocytochrome *c* as rapidly as does rCcP, *i.e.*, that electron transfer to Compounds I and II could be impaired.

The two mutations that have the most significant deviations from the correlation line in Figure S24 are E201K, and E290K. E290K increases K_M by more than 28-fold and it is reasonable to assume that this mutation alters the orientation of bound cytochrome *c* such that the rate of ferrocytochrome *c* oxidation is severely inhibited leading to the lower turnover rates.

The E201K mutation has the greatest effect on V_{max}/e_0, with an observed value of 2.8 ± 0.2 s^{-1}, less than 0.5 % of that of rCcP. We estimate that 42% of E201K reacts with hydrogen peroxide to form Compound I with a rate identical to that of rCcP, Table 3, indicating that the very low turnover number is related to oxidation of ferrocytochrome *c* and not the hydrogen peroxide reaction. The K_M value for E201K is within experimental error of K_M for rCcP suggesting that the E201K mutation does not alter the binding affinity for cytochrome *c*. This is consistent with the crystal structure of the yeast cytochrome *c*/CcP (1), which shows no significant electrostatic

interaction between Glu-201 and any of the positively-charged residues in bound cytochrome *c*. However, residue 201 is quite close to Ala-193 and Ala-194 on the surface of CcP, Figure 1, the putative entry point for electron transfer in the cytochrome *c*/CcP complex (1). It is possible that changing glutamate to lysine alters the exact orientation of the two proteins in the complex, slowing the rate of electron entry into CcP Compound I.

Four other mutants have intermediate deviations from the correlation line in Figure S24. D18K and E118K are about 40% below the line while E17K and E291K are about 40% above the line. E17K, D18K, and E291K don't affect the binding of cytochrome *c* and there is no apparent reason why these mutation should affect electron transfer from the bound cytochrome *c* to the Trp-191 radical in Compounds I and II. We are inclined to attribute the deviations of E17K, D18K, and E291K to errors in estimation of the amount of H_2O_2-inactive enzyme. On the other hand, the E118K mutation significantly affects the binding of cytochrome *c* and it is possible that the bound cytochrome *c* is in a different orientation that slows the rate of electron entry into CcP as suggested for the E201K mutation.

REFERENCES (For Supporting Information)

1. Pelletier, H., and Kraut, J. (1992) Crystal structure of a complex between electron transfer partners, cytochrome *c* peroxidase and cytochrome *c*, *Science 258*, 1748-1755.

2. Vitello, L. B., Huang, M., and Erman, J. E. (1990) pH-dependent spectral and kinetic properties of cytochrome *c* peroxidase: Comparison of freshly isolated and stored enzyme, *Biochemistry 29*, 4283-4288.

3. Yonetani, T., Wilson, D. F., and Seamonds, B. (1966) Studies on cytochrome *c* peroxidase. VIII. The effect of temperature on light absorptions of the enzyme and its derivatives, *J. Biol. Chem. 241*, 5347-5352.

4. Vitello, L. B., Erman, J. E., Mauro, J. M. and Kraut, J. (1990) Characterization of the hydrogen peroxide - enzyme reaction for two cytochrome *c* peroxidase mutants, *Biochim. Biophys. Acta 1038*, 90-97.

5. Dhaliwal, B. K., and Erman, J. E. (1985) A kinetic study of the alkaline transitions in cytochrome c peroxidase, *Biochim. Biophys. Acta 827*, 174-182.

6. Vitello, L. B., Erman, J. E., Miller, M. A., Mauro, J. M., and Kraut, J. (1992) Effect of asp-235 → asn substitution on the absorption spectrum and hydrogen peroxide reactivity of cytochrome *c* peroxidase, *Biochemistry 31*, 11524-11535.

7. Erman, J. E. (1976) Kinetic and equilibrium studies of cyanide binding by cytochrome *c* peroxidase, *Biochemistry 13*, 39-44.

8. Loo, S., and Erman, J. E. (1975) A kinetic study of the reaction between cytochrome *c* peroxidase and hydrogen peroxide. Dependence on pH and ionic strength, *Biochemistry 14*, 3467-3470.

9. Balny, C., Anni, H., and Yonetani, T. (1987) A stopped-flow study of the reaction of cytochrome *c* peroxidase with hydroperoxides, *FEBS Letts. 221*, 349-354.

10. Erman, J. E., Vitello, L. B., Mauro, J. M., and Kraut, J. (1989) Detection of an oxyferryl porphyrin π-cation radical intermediate in the reaction between hydrogen peroxide and a mutant yeast cytochrome *c* peroxidase. Evidence for tryptophan-191 involvement in the radical site of compound I, *Biochemistry 28*, 7992-7995.